THE JOURNAL OF BIOLOGICAL CHEMISTRY
Vol. 277, No. 25, Issue of June 21, pp. 22789–22797, 2002

Printed in U.S.A.

A Novel Zinc-regulated Human Zinc Transporter, hZTL1, Is Localized to the Enterocyte Apical Membrane*

Received for publication, January 18, 2002, and in revised form, April 5, 2002
Published, JBC Papers in Press, April 5, 2002, DOI 10.1074/jbc.M200577200

Ruth A. Cragg‡, Graham R. Christie§, Siôn R. Phillips‡, Rachel M. Russi‡, Sébastien Küry¶, John C. Mathers‡‖, Peter M. Taylor§, and Dianne Ford‡

From the ‖Human Nutrition Research Centre, ‡Department of Biological and Nutritional Sciences, University of Newcastle, Kings Rd., Newcastle upon Tyne, NE1 7RU, United Kingdom, §Division of Molecular Physiology, School of Life Sciences, MSI/WTB Complex, University of Dundee, Dundee, DD1 5EH, United Kingdom, and ¶Laboratoire d'Etude de Polymorphisme de l'ADN, Faculté de Médecine, 1, rue Gaston Veil, 44035 Nantes cedex, France

Zinc is essential to a wide range of cellular processes; therefore, it is important to elucidate the molecular mechanisms of zinc homeostasis. To date, no zinc transporters expressed at the enterocyte apical membrane, and so essential to mammalian zinc homeostasis, have been discovered. We identified hZTL1 as a human expressed sequence tag with homology to the basolateral enterocyte zinc transporter ZnT1 and deduced the full-length cDNA sequence by PCR. The protein of 523 amino acids belongs to the cation diffusion facilitator family of membrane transporters. Unusually, the predicted topology comprises 12 rather than 6 transmembrane domains. ZTL1 mRNA was detected by reverse transcription-PCR in a range of mouse tissues. A Myc-tagged hZTL1 clone was expressed in transiently transfected polarized human intestinal Caco-2 cells at the apical membrane. Expression of hZTL1 mRNA in Caco-2 cells increased with zinc supplementation of the nutrient medium; however, in the placental cell line JAR hZTL1 appeared not to be regulated by zinc. Heterologous expression of hZTL1 in *Xenopus laevis* oocytes increased zinc uptake across the plasma membrane. The localization, regulatory properties, and function of hZTL1 indicate a role in regulating the absorption of dietary zinc across the apical enterocyte membrane.

The involvement of zinc in a diverse array of cellular processes highlights the importance of understanding mechanisms of zinc homeostasis. Zinc is a catalytic and/or structural cofactor for several hundred metalloproteins, including zinc metalloenzymes and transcription factors. Central to cellular zinc homeostasis is likely to be the activity of membrane transporters that mediate cellular zinc uptake and efflux as well as intracellular zinc sequestration. To date, the identity of the zinc transporter most likely to play the major role in mammalian zinc homeostasis, the transporter expressed at the apical membrane of the enterocyte, has proved elusive. Most eukaryotic cDNAs cloned to date that encode proteins with zinc transport activity fall into one of two main groups.

The ZIP family of transporters, which included initially the yeast proteins ZRT1 (1), ZRT2 (2), and the *Arabidopsis* iron transporter IRT1 (3), now includes human proteins hZip1 and hZip2 (4, 5) plus *Arabidopsis* transporters Zip1–4 (6). The ability to mediate cellular zinc uptake appears to be a common function of this group of transporters. Consistent with a role in zinc uptake, the yeast high affinity transporter ZRT1 is induced by zinc restriction (1). All members listed above of this group of proteins share the same predicted topology; that is, eight membrane-spanning domains with extracellular N and C termini. Conserved histidine residues and polar or charged amino acids that lie close to these histidines in the predicted structure in transmembrane domains IV and V have been shown in IRT1 to be essential for transport function (7).

The properties and localization of members of a second group of proteins, the cation diffusion facilitator (CDF)[1] family, are consistent with a role in zinc efflux or intracellular sequestration in vesicles/vacuoles. Most genes in this diverse family, which is defined by a specific sequence motif (8), were cloned as a result of conferring resistance to transition metal toxicity. The CDF family includes ZRC1, which confers zinc resistance in yeast (9), and COT1, a yeast cobalt transporter (10), plus the mammalian proteins ZnT1–4 (11–14). Common to most members of the CDF family is a predicted transmembrane structure comprising six membrane-spanning domains with intracellular N and C termini and, in the case of eukaryotic members, a histidine-rich intracellular loop that represents a potential zinc binding region (8). Although the published data are consistent with a direct role for mammalian CDF-family transporters in mediating zinc transport, this has not been demonstrated directly by expression in a heterologous system. It remains a possibility that CDF-family transporters are auxiliary factors in zinc transport or subunits of a larger zinc transporter complex (11). Consistent with a role in zinc transport are the regulatory properties of ZnT1 and ZnT2. A severely zinc-restricted diet led to reduced levels of ZnT2 mRNA expression in rat kidney and intestine, whereas a diet supplemented with zinc or a single oral dose of zinc led to increased abundance of ZnT1 and ZnT2 mRNAs in both tissues (15).

There has been debate over a role for the divalent cation transporter DMT1 (also referred to as Nramp2 or DCT1) in cellular zinc uptake. Heterologously expressed rat DMT1 has

* This work was funded by Biotechnology and Biological Sciences Research Council (BBSRC) Grant 13/D11912 (to D. F. and J. C. M.), by an award from the Faculty of Agriculture and Biological Sciences, University of Newcastle (to R. A. C.), and by a BBSRC studentship (to R. M. R.). The costs of publication of this article were defrayed in part by the payment of page charges. This article must therefore be hereby marked "*advertisement*" in accordance with 18 U.S.C. Section 1734 solely to indicate this fact.

The nucleotide sequence(s) reported in this paper has been submitted to the GenBank™/EBI Data Bank with accession number(s) AF439324.

** To whom correspondence should be addressed. Tel.: 44-191-2225986; Fax: 44-191 2228684; E-mail: dianne.ford@ncl.ac.uk.

[1] The abbreviations used are: CDF, cation diffusion facilitator; RACE, rapid amplification of cDNA ends; AE, acrodermatitis enteropathica; MRE, metal response element; RT, reverse transcriptase; Tricine, *N*-[2-hydroxy-1,1-bis(hydroxymethyl)ethyl]glycine; UTR, untranslated region; MTF1, MRE-binding transcription factor 1.

been demonstrated to mediate proton-coupled uptake of Fe^{2+} into *Xenopus laevis* oocytes, and the divalent cations Fe^{2+}, Zn^{2+}, Cd^{2+}, Mn^{2+}, Cu^{2+}, Co^{2+}, Ni^{2+}, and Pb^{2+} all evoked inward currents in this expression system (16). However, it has since been established that Fe^{2+} and Zn^{2+} are transported across the apical membrane of the intestinal Caco-2 cell line by distinct mechanisms. Zinc did not inhibit DMT1-mediated Fe^{2+} uptake in this system nor was Zn^{2+} uptake affected by reduced expression of DMT1 (17). Furthermore, whereas DMT1-mediated transport is coupled to proton co-transport, uptake of zinc by small intestinal brush border membrane vesicles was inhibited by an inwardly directed H^+ gradient (18).

Transport of zinc by the enterocyte from the gut lumen to the blood is essential to mammalian zinc homeostasis. The symptoms of the zinc deficiency disease acrodermatitis enteropathica (AE), a rare autosomal recessive genetic abnormality, result from zinc malabsorption (19). ZnT-1, expressed at the basolateral membrane (20), may be involved in mediating zinc transport from enterocyte to blood. ZnT-4 is expressed in rat intestine in the membrane of intracellular vesicles (21) and ZnT-2, whose RNA can be detected in intestine, is similarly localized in baby hamster kidney cells (12) and probably, therefore, also in intestine. ZnT3 is expressed only in brain and testis (13). HZIP1, localized to the plasma membrane in K562 erythroleukemia cells (4), has recently been demonstrated to have a vesicular localization in the human intestinal Caco-2 cell line (22), ruling out a role in mediating zinc transport across the enterocyte brush border membrane. HZIP2 has been detected only in prostate and uterus (5). To our knowledge, it has yet to be demonstrated that any of the ZIP or CDF family zinc transporters cloned to date are localized at the apical enterocyte membrane. The human natural resistance-associated macrophage protein 1 (Nramp1) shows a high degree of homology to DMT1 and is a functional zinc transporter (23). However, Nramp1 is expressed exclusively in macrophages (24). Thus, the identity of the transporter primarily responsible for dietary zinc uptake in mammals remains unknown.

We report the cloning of a novel human zinc transporter expressed at the apical membrane of the Caco-2 human small intestinal cell line model, whose sequence places it within the CDF family but which has apparently different topology from the other cloned mammalian members. We propose that this protein represents the first member of a new subfamily of mammalian zinc transporters and refer to the transporter as hZTL1 (human ZnT-Like transporter 1). We show mouse ZTL1 to have widespread tissue distribution and demonstrate differential regulation by zinc of hZTL1 mRNA expression levels in cultured intestinal and placental cell lines. We present data confirming the predicted functional activity of hZTL1 with respect to zinc transport.

EXPERIMENTAL PROCEDURES

Rapid Amplification of cDNA Ends (RACE)—A pair of nested reverse primers, ^{286}GTTTGGATGGTTCATCGCTGACCCAC^{261} and ^{197}GCCAGGTTCTACTCCTGAGATTGCCACC^{170}, annealing to an EST (GenBank™ accession number AA993841) identified through homology at the protein level to mouse ZnT1, was designed and used for 5′-RACE. 5′-RACE was carried out from human small intestine Marathon-Ready™ cDNA (CLONTECH) following the manufacturer's instructions and using the Advantage cDNA polymerase mix (CLONTECH) as recommended. Thermal cycling parameters for the first round of amplification were: 94 °C for 30 s; 5 cycles at 94 °C for 5 s, 72 °C for 4 min; 5 cycles at 94 °C for 5 s, 70 °C for 4 min; 25 cycles at 94 °C for 5 s, 68 °C for 4 min. Cycling parameters were the same for the nested reaction, but the final cycle number was reduced to 20.

The product, ~2 kb in size, was subcloned into the vector pCR2.1 TOPO (Invitrogen) for sequencing. Sequencing was carried out by the Molecular Biology Facility, University of Newcastle using an ABI Prism model 377 automated sequencer.

RNA Preparation—RNA was prepared from cells and tissues using RNAzol B (Biogenesis) following the manufacturer's instructions.

Generation of an hZTL1 cDNA Clone—A cDNA clone of hZTL1 coding for all but the 42 C-terminal-most amino acids was generated by nested RT-PCR from Caco-2 mRNA. Reverse transcription was for 2 h at 42 °C using Moloney murine leukemia virus reverse transcriptase (Invitrogen) (2 units/μl) in the manufacturer's buffer (50 mM Tris-HCl (pH 8.3), 50 mM KCl, 4 mM $MgCl_2$) containing 1 mM dithiothreitol, 0.5 mM dNTPs, 0.001 units/μl hexanucleotide primer, and 1.5 units/μl ribonuclease inhibitor. Reactions were terminated by heating to 95 °C for 5 min, and cDNA was amplified initially over 30 cycles (94 °C for 30 s, 50 °C for 30 s, 72 °C for 90 s) in a PCR reaction mixture containing 0.2 mM dNTPs, 0.5 mM each primer (^{670}GCTGTGATCTGTTTATTGC^{688} and ^{2274}GGTTGTCTGTTTTACTTCCAG^{2254}), and 1× Advantage cDNA polymerase mix (CLONTECH) in the manufacturer's buffer (40 mM Tricine-KOH (pH 9.2), 15 mM potassium acetate, 3.5 mM magnesium acetate, 3.75 μg/ml bovine serum albumin). The nested PCR reaction was as for the first round of amplification but using the primer pair ^{694}GACAATGATGATCTCATGGC^{713} and ^{2152}GCAATCTCAGGAGTAGAAC^{2134} and an annealing temperature of 56 °C. The 1459-bp cDNA fragment was sub-cloned into the vector pCR2.1 TOPO (Invitrogen) to give the plasmid pZTL1–50. The sequence of the clone was confirmed as above. Attempts to generate a clone that included the entire C-terminal region were unsuccessful.

Northern Blotting—Twenty micrograms of total RNA prepared from Caco-2 cells were run on a 1.2% formaldehyde-containing agarose gel, transferred to a nylon membrane (Hybond N, Amersham Biosciences) by capillary electrophoresis, and fixed by UV cross-linking. The membrane was prehybridized at 42 °C in 50% formamide, 2× SSPE (300 mM NaCl, 20 mM NaH_2PO_4, 2 mM EDTA (pH 7.4)), 5× Denhardt's reagent, 0.5% (w/v) SDS, 100 μg/ml sonicated salmon sperm DNA (Sigma) and then hybridized for 16 h in the same buffer containing 25 ng of ^{32}P-labeled cDNA probe. The probe comprised the 1521-bp fragment including the hZTL1 cDNA sequence removed using *Eco*RI from pZTL1–50. The membrane was washed at 65 °C in 2× SSC (300 mM NaCl, 30 mM sodium citrate), 0.1% SDS and examined by electronic autoradiography using a Packard Instant Imager.

Sequencing of hZTL1 in AE Patients—The group of 20 AE patients who form the basis of this study was recruited from 12 families from France and Tunisia. Each patient was individually examined by an experienced dermatologist to confirm the diagnosis of AE. After obtaining informed consent, anticoagulated venous blood was sampled from each patient and used for direct DNA preparations. High molecular weight genomic DNA was isolated using the Nucleon BACC2 kit according to the manufacturer's protocol (Amersham Biosciences). For each of the 20 AE patients, the 11 exons of hZTL1 were PCR-amplified using 20 ng of genomic DNA per reaction, and primers were designed in the flanking intronic regions at 50 bp or more from the splice sites. PCR amplifications were initiated by a denaturation of 10 min at 94 °C followed by 5 cycles of 45 s at 94 °C, 20 s at 5 °C over the annealing temperature and 90 s at 72 °C then by 25 cycles of 45 s at 94 °C, 20 s at annealing temperature and 90 s at 72 °C with a final extension at 72 °C for 10 min. PCR products were sequenced automatically (ABI 377 sequencing system using Thermo Sequenase II Dye Terminator cycle sequencing premix kit, Amersham Biosciences).

Culture of Mammalian Cells—Caco-2 cells (passage 30) were seeded into 25-cm^2 flasks at a density of approximately one million cells per flask and maintained at 37 °C in a humidified atmosphere of 5% CO_2 in air in Dulbecco's modified Eagle's medium (with 4.5 g/liter glucose) supplemented with 10% (v/v) fetal calf serum, 60 μg/ml gentamycin, 2 mM L-glutamine, and 1% (v/v) nonessential amino acids. All tissue culture reagents were supplied by Sigma. The medium was replaced twice weekly. For growth at increased concentrations of zinc, $ZnCl_2$ was added to the culture medium, progressively increasing the concentration from 3 μM (standard medium, measured using a Unicam 701 inductively coupled plasma optical emission spectrometer) to 20, 50, and, finally, 100 μM. This approach was necessary because $ZnCl_2$ at 100 μM added to non-conditioned cells proved toxic. For growth at 20 μM $ZnCl_2$, the salt was added to a confluent cell monolayer (14 days post-seeding) for 7 days before passaging cells by the addition of 0.05% (w/v) trypsin, 0.2% EDTA in Earle's balanced salt solution (Sigma). Newly seeded cells were then maintained for a further 7 days at 20 μM $ZnCl_2$ before increasing the $ZnCl_2$ concentration to 50 μM. Cells were passaged after an additional 7 days of growth and maintained for a further 7 days at 50 μM $ZnCl_2$. The $ZnCl_2$ concentration of the nutrient medium was then increased to 100 μM and cells were maintained at this concentration for 7 days before harvesting RNA.

JAR cells were cultured as described above for Caco-2 cells with a

number of modifications. Nutrient medium comprised RPMI 1640 (Invitrogen) supplemented with 2 mM L-glutamine, 10% fetal calf serum, and penicillin/streptomycin (100 units/ml and 100 μg/ml, respectively). Seeding density was 2.5×10^6 cells/cm^2. Cells were passaged every 7 days. JAR cells were able immediately to tolerate $ZnCl_2$ added to the nutrient medium at a concentration of 100 μM. $ZnCl_2$ was added to cells 1 day post-seeding, and cells were maintained in this medium for 6 days before harvesting RNA.

Detection of hZTL1 Localization by Transient Transfection of Caco-2 Cells—A construct for the expression in mammalian cells of hZTL1 tagged at the C terminus with the Myc epitope was produced by *Eco*RI digestion of plasmid pZTL1–50 followed by ligation of the gel-purified (Nucleospin kit, CLONTECH) 1476-bp fragment into the plasmid pCDNA3.1/Myc-His A (Invitrogen) to give the plasmid pZTL1-Myc.

For transfection, Caco-2 cells were seeded at a density of 5×10^5 cells/cm^2 onto polycarbonate tissue culture inserts (0.4-μm pore, 12-mm diameter, Costar) and cultured for 14 days until differentiated. The plasmid pZTL1-Myc was precipitated by the addition of 1 μg DNA in 250 mM $CaCl_2$ to an equal volume of HEPES-buffered saline (pH 7.05; 280 mM NaCl, 50 mM HEPES, 1.5 mM Na_2HPO_4). A 400 μl volume of this mixture was then added to cells in 3 ml of complete nutrient medium in the upper chamber only. Medium was then removed after 8 h, and cells were treated with 10% glycerol in complete medium for 4 min. Cells were washed twice in phosphate-buffered saline and maintained in complete medium for 48 h. Cells were fixed for 5 min in methanol at room temperature. The hZTL1-fused Myc epitope was detected using fluorescein isothiocyanate-conjugated anti-Myc antibody (Invitrogen) following the manufacturer's instructions. Nuclei were stained by incubation with 5 μg/ml propidium iodide in phosphate-buffered saline for 5 min, and cells were then mounted in Vectashield fluorescence mounting medium (Vector Laboratories Ltd). The pattern of fluorescence was visualized by confocal laser-scanning microscopy.

Semi-quantitative RT-PCR—Co-amplification of hZTL1 or metallothionein mRNA and 18 S rRNA was carried out using the GeneAmp RNA PCR core kit (Applied Biosystems) following the manufacturer's instructions and using either the hZTL1-specific primers ^{1939}GGTGGAGGCATGAATGCTA^{1957} and ^{2160}TTCTGGCAATCTCAGG^{2142} or the metallothionein-specific primers ^{24}ATGGACCCAACTGCTCC^{41} and ^{209}TCAGGCACAGCAGCTGCAC^{191} (GenBank™ accession number XM_048212) along with 18 S rRNA-specific primers (Ambion) with thermal cycling parameters: 95 °C, 30 s; 57 °C, 30 s; 72 °C, 60 s for hZTL1 amplification and 95 °C, 30 s; 59 °C, 30 s; 72 °C, 90 s for metallothionein amplification. PCR cycle number was limited to within an experimentally determined linear range of amplification (35 cycles for hZTL1; 33 cycles for metallothionein). 18 S rRNA primers modified at their 3′ end so as to render them non-extendable (Classic Quantum RNA 18 S Internal Standards, Ambion) were also included in the reaction at an appropriate ratio determined empirically to reduce the intensity of the 18 S rRNA band (when viewed after agarose gel electrophoresis) to within the range of the hZTL1 band and thus enable accurate normalization of the hZTL1-specific product against 18 S rRNA.

In Vitro Transcription of hZTL1 cRNA—The plasmid pZTL1–50 was linearized 3′ of the hZTL1 insert using the restriction endonuclease *Sst*I. Complementary RNA was transcribed from the T7 promoter upstream of the hZTL1 cDNA using the mMessage mMachine kit (Ambion) following the manufacturer's instructions.

Measurement of hZTL1 Activity in X. laevis Oocytes—Oocytes (stage V or VI) were isolated from ovarian tissue obtained from mature female *X. laevis* toads (S. African *Xenopus* facility) as described previously (25). Tissue was digested with 2 mg/ml collagenase A (Roche Molecular Biochemicals) in Ca^{2+}-free modified Barth's medium (88 mM NaCl, 1 mM KCl, 2.4 mM $NaHCO_3$, 0.82 mM $MgSO_4$, 20 mM HEPES/Tris (pH 7.6), 10 mg/ml gentamycin) at 22 °C for 3 h with gentle agitation. Oocytes were injected with 50 nl of either deionized water or hZTL1 cRNA (2 μg/ml) and left for 3 days at 18 °C in modified Barth's medium (88 mM NaCl, 1 mM KCl, 2.4 mM $NaHCO_3$, 0.82 mM $MgSO_4$, 0.33 mM $Ca(NO_3)_2$, 0.41 mM $CaCl_2$, 20 mM HEPES/Tris (pH 7.6), 10 mg/ml gentamycin) before measurement of zinc fluxes across the oocyte plasma membrane. Zinc uptake into injected oocytes was measured by incubating groups of 10–15 oocytes for 2 or 4 h in 300 μl of modified Barth's medium plus 12 μM $ZnCl_2$ including 6.4 μCi/ml $^{65}Zn^{2+}$ (PerkinElmer Life Sciences). Oocytes were washed 3 times in deionized water before measuring $^{65}Zn^{2+}$ incorporation into single oocytes using a γ counter.

Bioinformatics Tools—Sequence alignments were performed using BLAST (26). A putative transmembrane topology for hZTL1 was derived using TMpred, an algorithm based on statistical analysis of the TMbase data base of naturally occurring transmembrane protein segments using maximum and minimum values of 29 and 19, respectively, for the length of the hydrophobic region of the membrane helix (27). Analysis of the hZTL1 peptide sequence for conserved motifs, *O*-glycosylation sites, and signal peptide sequences was by the use of InterProScan (28), NetOglyc (29), and SignalP (30) respectively. Genomic sequence between regions corresponding to the hZTL1 cDNA clone was screened for additional exons using FGENE (31) and FEX (32).

RESULTS

The Sequence and Gene Structure of a Novel Zinc Transporter, hZTL1—The cDNA sequence of a putative novel zinc transporter identified initially as a 3′ EST with homology at the protein level to ZnT1 was determined by 5′-RACE from a human intestinal cDNA library. Assuming the first in-frame ATG codon to be the start of translation, the open reading frame codes for a protein of 523 amino acids (Fig. 1*A*) and the cDNA clone includes 708 bp of the 5′-untranslated region. The sequence around the ATG at position 709, however (CTCATGG), deviates from the Kozak consensus sequence (R*XX*ATGG), whereas a second in-frame ATG at position 718 (AAAATGG) concurs with the Kozak consensus sequence. Translation from this potential start codon would produce a protein truncated at the N terminus by three amino acids in comparison to the sequence we state. Amino acid residues 271–287 (Fig. 1*B*) comprise the CDF signature sequence (8), thus placing this protein within the CDF family. Topology prediction using TMpred (or alternatively, TMAP (33)) indicates 12 membrane-spanning domains with extracellular N and C termini and a histidine-rich intracellular loop, potentially involved in zinc binding, between transmembrane domains IX and X. This conformation is favored over a possible alternative with cytoplasmic N and C termini both by comparison with the TMbase data base of naturally occurring transmembrane protein segments (27) and by homology with ZnT family members. HZTL1 shows 34% identity to ZnT1 over a stretch of 122 amino acids (Fig 1*B*). The region of homology spans transmembrane domains I- IV in ZnT1 and domains VI-IX in hZTL1 (Fig. 1*C*). Intracellular N and C termini would reverse the orientation of the transmembrane domains in hZTL1 with respect to their homologous domains in ZnT1 and, furthermore, would position the histidine-rich loop in an uncharacteristic extracellular position. The region best conserved across all members of the CDF family encompasses transmembrane domains I- IV of the typical, six-transmembrane domain structure (8). Identity between hZTL1 and other members of the ZnT family is as follows; for rat ZnT2, 22% over a region 239 amino acids in length; for mouse ZnT3, 21% identity over a stretch of 244 amino acids; for mouse ZnT4, 25% identity over a region of 252 amino acids. As for ZnT1, this homology is due to alignment of transmembrane domains I- IV in the ZnT transporters with transmembrane domains IV- IX of hZTL1 but also due to homology between transmembrane domains V and VI of the ZnT transporters and transmembrane domains X and XI of hZTL1. Analysis of the amino acid sequence of hZTL1 reveals no nucleotide binding motifs, no predicted sites for *O*- or *N*-glycosylation, and no apparent signal peptide or mitochondrial targeting sequence.

Alignment of the hZTL1 cDNA sequence with the draft human genome sequence localizes the gene on chromosome 5 (position 77269K-77651K). The deduced gene structure is shown in Fig. 2. The appearance on a Northern blot of Caco-2 RNA probed with hZTL1 cDNA of two bands (Fig. 2*C*) suggests alternatively spliced hZTL1 transcripts. Analysis of the inter-exon sequence on chromosome 5 indicates no additional potential exons between exons 3 and 11. However, the regions designated introns 1 and 2 include additional potential coding sequence, possibly suggesting N-terminal splice variants. It is

A

```
1                                                  50                                                 100
MAKMAEHPEGHHDSALTHMLYTAIAFLGVADHKGGVLLLVLALCCKVGFHTASRKLSVDVGGAKRLQALSHLVSVLLLCPWVIVLSVTTESKVESWFSLI
                                I                                                  II

                                                  150                                                200
MPFATVIFFVMILDFYVDSICSVKMEVSKCARYGSFPIFISALLFGNFWTHPITDQLRAMNKAAHQESTEHVLSGGVVVSAIFFILSANILSSPSKRGQK
   III                                  IV                                                 V

                                                  250                                                300
GTLIGYSPEGTPLYNFMGDAFQHSSQSIPRFIKESLKQILEESDSRQIFYFLCLNLLFTFVELFYGVLTNSLGLISDGFHMLFDCSALVMGLFAALMSRW
                                                        VI                                  VII

                                                  350                                                400
KATRIFSYGYGRIEILSGFINGLFLIVIAFFVFMESVARLIDPPELDTHMLTPVSVGGLIVNLIGICAFSHAHSHAHGASQGSCHSSDHSHSHHMHGHSD
                          VIII                                  IX

                                                  450                                                500
HGHGHSHGSAGGGMNANMRGVFLHVLADTLGSIGVIVSTVLIEQFGWFIADPLCSLFIAILIFLSVVPLIKDACQVLLLRLPPEYEKELHIALEKVLYVI
                                X                                   XI

                          523
SSLLSSLKITFLKSLLEVKQTTK
      XII
```

B

```
hZTL1: 247 QIFYFLCLNLLFTFVELFYGVLTNSLGLISDGFHMLFDCSALVMGLFAALMS-RWKATRI 305
           ++   L L  +F  +E+    +T SL ++SD FHML D  ALV+ L A   + R  AT+
mZnT-1: 10 RLLCMLLLTFMFMVLEVVVSRVTASLAMLSDSFHMLSDVLALVVALVAERFARRTHATQK 69

hZTL1: 306 FSYGYGRIEILSGFINGLFLIVIAFFVFMESVARLIDPPELDTHMLT-PVSVGGLIVNLI 364
            ++G+ R E++   +N +FL  + F + +E+V R I+P E+   ++   V V GL+VN++
mZnT-1:70  NTFGWIRAEVMGALVNAIFLTGLCFAILLEAVERFIEPHEMQQPLVVLSVGVAGLLVNVL 129

hZTL1: 365 GI 367
           G+
mZnT-1:130 GL 131
```

C

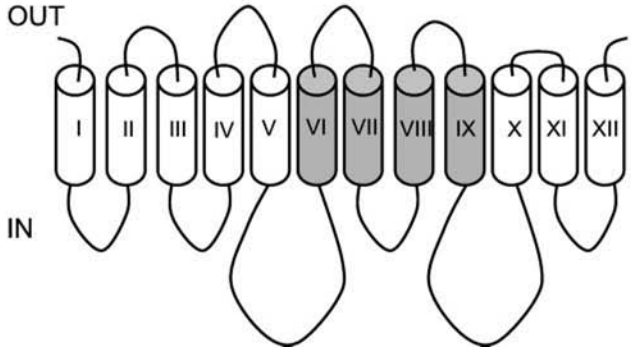

FIG. 1. **The hZTL1 amino acid sequence and predicted topology.** *A*, theoretical translation of the hZTL1 cDNA sequence (GenBank™ accession number AF39324), indicating the 12 predicted transmembrane regions. *B*, alignment of the hZTL1 amino acid sequence with the sequence of mouse ZnT1. The CDF signature sequence is *underlined*. *C*, the predicted transmembrane topology of hZTL1. The *shaded area* indicates the region of homology with ZnT1.

also possible that additional exons 3′ of exon 11 contribute to the larger transcript. The TATA box consensus sequence TATAAAA lies 71 nucleotides upstream of the 5′ end of the hZTL1 cDNA clone. This putative TATA box, an element that is characteristically centered ~25 bases upstream of the start of transcription, possibly indicates that the 5′-UTR of the cDNA clone is incomplete. The promoter region of the *hZTL1* gene includes core, consensus metal response element (MRE) sequences (TGCRCNC) centered at positions 461, 645, 1238, 2257, and 3250 nucleotides upstream of the start of the cDNA sequence. The sequences at positions −645 and −3250 are in the forward orientation, whereas those at −461, −1238, and −2257 are in the reverse orientation. MRE binding transcription factor 1 (MTF-1) is known to regulate basal and zinc-induced expression of metallothionein in cultured cells (34) and to mediate zinc induction of metallothionein expression in visceral endoderm cells during early development *in utero* of the mouse (35).

A recent report placing the AE locus in the majority of patients analyzed (from Jordanian and Egyptian populations) on chromosome 8 (36) excludes the possibility that a mutation in hZTL1 is responsible for the disease in these subjects. However, for two cases in this study the AE syndrome appeared not to be linked to the same locus (36); thus, it is possible that other loci are responsible for some forms of AE. We therefore investigated the possibility that a mutation in hZTL1 might account for the symptoms of AE in patients not carrying the disease-linked markers on chromosome 8. Three SNPs in the coding

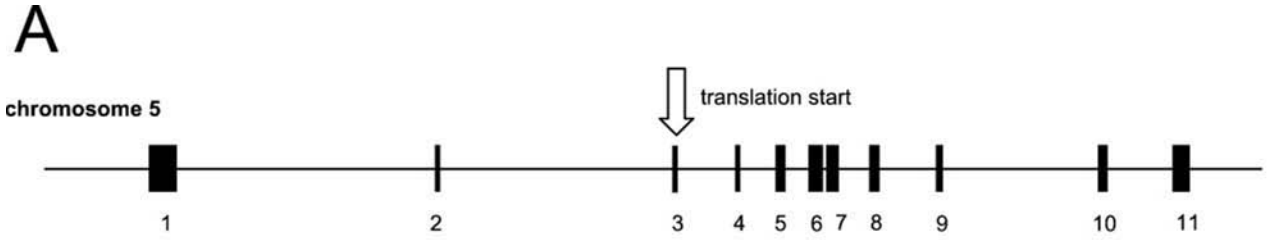

B

Exon structure

exon no.	size (bp)	nucleotide nos.
1	554	1-554
2	88	555-642
3	88	643-730
4	77	731-807
5	171	808-978
6	289	979-1267
7	209	1268-1476
8	158	1477-1634
9	130	1635-1764
10	202	1765-1966
11	342	1967-2308

Intron structure

intron no.	size (bp)
1	5220
2	4703
3	1192
4	740
5	518
6	179
7	636
8	1102
9	3065
10	1303

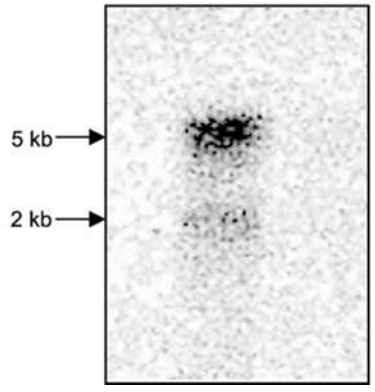

FIG. 2. **The hZTL1 gene structure.** *A*, alignment of the *hZTL1* gene on chromosome 5. Heavy regions indicate exons (*numbered*). The position of the start of translation (in intron 3) is indicated. *B*, the exon and intron structure of the *hZTL1* gene based on the alignment shown in *panel A*. *C*, a Northern blot of Caco-2 RNA probed with hZTL1 cDNA. The approximate sizes of hybridizing transcripts are indicated.

region were noted (2 in exon 10, and 1 in exon 11); however, none result in amino acid substitutions, and none correspond to presence of the disease. Thus, we exclude the possibility that a mutation in hZTL1 accounts for AE in the 12 families examined in the present study. However, we cannot exclude definitively that hZTL1 may be the molecular cause of AE for other unrelated families diagnosed with this disorder.

Expression Profile of hZTL1 in Mouse Tissues—ZTL1 mRNA was detected by RT-PCR in all mouse tissues analyzed. Fig. 3*A* shows the relative levels of expression of hZTL1 mRNA in these tissues. We detected a difference in expression of ~4-fold relative to 18 S rRNA between kidney, a tissue expressing ZTL1 mRNA at relatively high levels, and liver, which expresses a relatively low level.

Subcellullar Localization of hZTL1—The localization of hZTL1 in a confluent monolayer of Caco-2 cells maintained in culture for 14 days to ensure differentiation was determined by confocal laser-scanning microscopy to visualize a fluorescein isothiocyanate-conjugated anti-Myc antibody after transfection with a construct from which hZTL1 was expressed as a fusion protein with the Myc epitope at the C terminus. A series of sections parallel to the plane of the monolayer (a Z-series; Fig. 3*B*) and a section through a transfected cell perpendicular to the monolayer (an XZ-section; Fig. 3*C*) demonstrate clearly apical localization of anti-Myc immunoreactivity. Thus apical localization of hZTL1 in the human enterocyte is indicated.

Regulation by Zinc of hZTL1 Expression Levels—The effect of zinc availability on levels of expression of hZTL1 mRNA in human intestinal Caco-2 cells was determined by culturing cells at progressively increasing concentrations of zinc until cells were able to tolerate 100 μM $ZnCl_2$. The zinc concentration of standard nutrient medium was determined as 3 μM by inductively coupled plasma optical emission spectroscopy. After 7 days of growth in 100 μM $ZnCl_2$, cells expressed hZTL1 mRNA at levels more than 2-fold greater than co-passaged controls (Fig. 4*A*). Regulation by zinc of hZTL1 mRNA expression in the human placental cell line JAR was also studied. Unlike Caco-2 cells, JAR cells were able to immediately tolerate an increase in the $ZnCl_2$ concentration of the nutrient medium from 3 to 100 μM. We found that culturing JAR cells for 7 days at 100 μM rather than 3 μM $ZnCl_2$ resulted in no change in hZTL1 mRNA levels (Fig. 4*B*). In both cell lines, levels of metallothionein mRNA, known to be regulated by zinc (34), were increased at 100 μM compared with 3 μM $ZnCl_2$ (Fig. 4, *C* and *D*).

Functional Activity of hZTL1—The ability of hZTL1 to mediate zinc transport into the cell was determined by functional expression in *X. laevis* oocytes. Uptake of $^{65}Zn^{2+}$ into oocytes showed a progressive increase over periods of at least 4 h (Fig. 5*A*, *inset ii*). The rate of uptake of $^{65}Zn^{2+}$ supplied at 12 or 50 μM into oocytes injected with hZTL1 cRNA was significantly greater than into water-injected controls (Fig. 5*A*) over a 4-h period and was markedly inhibited by excess (10 mM) unlabeled $ZnCl_2$ in the uptake medium, demonstrating a saturable process. An increase in uptake at 50 μM compared with 12 μM Zn^{2+} demonstrates a relatively high K_m. Assuming an oocyte volume of 500 nl, the uptake of Zn^{2+} at the rate measured would potentially lead to an increase in intracellular Zn^{2+} concentration after 4 h of 150 μM. Thus Zn^{2+} uptake appears to be accumulative.

The rate of $^{65}Zn^{2+}$ uptake into both hZTL1 cRNA-injected oocytes and water-injected controls was reduced at pH 5.5 compared with pH 7.6 (Fig. 5*B*). We observe that endogenous Zn^{2+} uptake is more sensitive to inhibition at acid pH (5.5) than hZLT1-mediated Zn^{2+} uptake, indicating that the two mechanisms are functionally distinct. It also appears that hZTL1-mediated $^{65}Zn^{2+}$ uptake is marginally favored at higher pH (Fig. 5*B*). The slope of the plot of hZTL1-mediated $^{65}Zn^{2+}$ uptake against pH is significantly greater than zero ($p < 0.05$

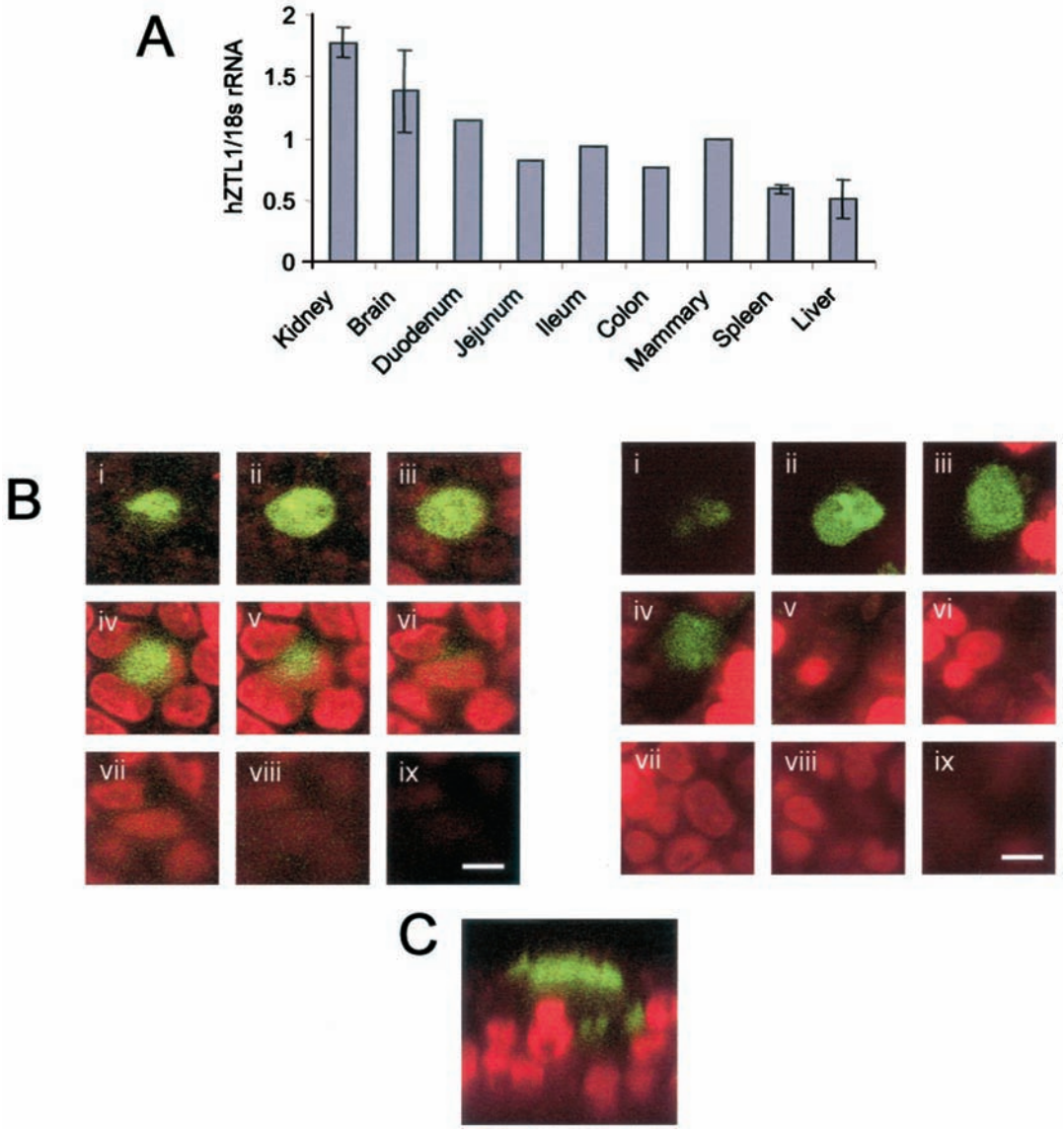

FIG. 3. **Localization of hZTL1.** *A*, relative levels of hZTL1 mRNA in a range of mouse tissues, expressed as a ratio of 18 S rRNA levels, determined by semi-quantitative RT-PCR. Where *error bars* (S.D.) are included, values shown are the means of two independent experiments. *B*, representative Z-series through Caco-2 monolayers transfected with hZTL1 cDNA tagged at the C terminus with the Myc epitope and probed with fluorescein isothiocyanate-conjugated anti-Myc antibody (*green*). Red staining indicates nuclei stained with propidium iodide. *Panels i* through *ix* show a series of sections through the monolayer passing from the apical to basolateral surface. The two series are from independent experiments. *Scale bar* = 10 μm. *C*, an XZ section through a Caco-2 monolayer transfected with hZTL1 cDNA tagged at the C terminus with the Myc epitope and probed with fluorescein isothiocyanate-conjugated anti-Myc antibody (*green*). Red staining indicates nuclei stained with propidium iodide. The *top* of the panel is closest to the apical membrane. *Scale bar* = 10 μm.

by linear regression analysis), confirming uptake to be a pH-dependent process.

DISCUSSION

We report the cloning of a novel zinc transporter whose sequence places it within the CDF family of metal ion transporters and which includes 12 putative transmembrane domains. Although a six-transmembrane domain structure is characteristic of CDF family proteins, a predicted structure that includes 12 membrane-spanning domains is not without precedent. The product of the yeast *MSC2* gene, which belongs to the CDF family and has recently been demonstrated to affect cellular distribution of zinc (37), is also predicted to have 12 transmembrane domains. Homology with the other cloned mammalian CDF proteins is such that hZTL1 might be regarded as a ZnT-type protein with an N-terminal extension of five transmembrane domains. Interestingly, evidence based on the properties of ZnT1 deletion mutants indicates that ZnT1 is functional only as a multimer (11). It is therefore reasonable to speculate that the N-terminal extension on hZTL1 might allow functionality in the monomeric form.

Expression of hZTL1 tagged with the Myc epitope localized to the apical membrane of human intestinal Caco-2 cells. The Caco-2 cell line shows features typical of the enterocyte including polarized localization to the appropriate membranes of a number of proteins (38–40). We conclude, therefore, that hZTL1 also localizes to the brush border membrane of the enterocyte *in vivo*.

We observed that increasing the Zn^{2+} concentration of the nutrient medium from 3 to 100 μM resulted in up-regulation of hZTL1 mRNA levels in human intestinal Caco-2 cells but not in the human placental cell line JAR. The region upstream of the hZTL1 cDNA sequence on chromosome 5 includes core consensus MREs at positions −461, −645, −1238, −2257, and −3250. Expression of hZTL1 may be regulated in Caco-2 cells by the binding of the transcription factor MTF1 (34) to these MREs.

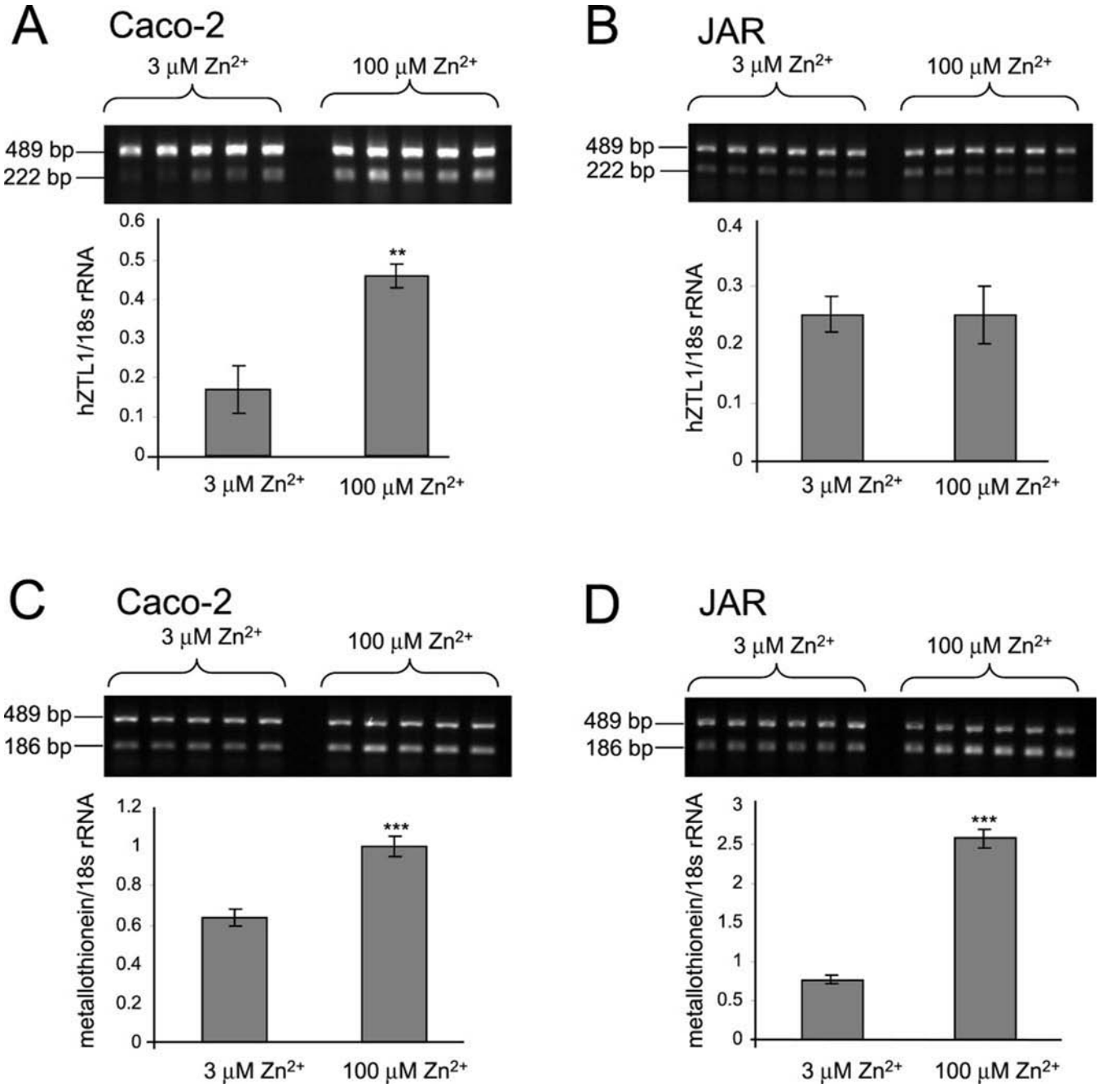

FIG. 4. **Regulation by zinc of hZTL1 and metallothionein mRNA levels in Caco-2 and JAR cells.** Histograms were obtained by densitometric measurement of band intensities from the ethidium bromide-stained agarose gels shown above each. Bands were generated by semi-quantitative RT-PCR from RNA samples extracted from cells grown in the presence of either 3 μM Zn^{2+} or 100 μM Zn^{2+} as indicated. Negative control RT-PCR reactions identical to those yielding the products shown except for the omission of Moloney murine leukemia virus reverse transcriptase resulted in no products. *A*, analysis of relative hZTL1 mRNA levels (222 bp) expressed as a ratio of 18 S rRNA levels (489 bp) in Caco-2 cells; **, $p < 0.01$, Student's *t* test. *B*, analysis of relative hZTL1 mRNA levels (222 bp) expressed as a ratio of 18 S rRNA levels (489 bp) in JAR cells. *C*, analysis of relative metallothionein mRNA levels (186 bp) expressed as a ratio of 18 S rRNA levels (489 bp) in Caco-2 cells; ***, $p < 0.001$, Student's *t* test. *D*, analysis of relative metallothionein mRNA levels (186 bp) expressed as a ratio of 18 S rRNA levels (489 bp) in JAR cells; ***, $p < 0.001$, Student's *t* test.

The more proximal MREs are stronger candidates for mediating zinc-regulated gene expression because of the proximal location of the multiple MREs in the MTF1-regulated metallothionein and ZnT1 genes (34, 41). The molecular basis for the apparent differential sensitivity to zinc of hZTL1 expression in intestine and placenta will be the subject of further study.

Without knowledge of the localization of hZTL1 in placenta, one can only speculate on the rationale behind the different regulatory responses of the *hZTL1* gene in the two tissues to changes in zinc availability. In intestine, increased levels of hZTL1 expression in response to increased zinc availability might facilitate more efficient uptake from a rich dietary supply. Tight homeostatic control of maternal circulating zinc concentration through regulated intestinal zinc absorption and by mobilization from tissue stores may render unnecessary any regulation by zinc availability of placental zinc transport.

Functional expression of hZLT1 in *X. laevis* oocytes is indicated by measurement of increased uptake of $^{65}Zn^{2+}$ in oocytes injected with hZTL1 cRNA, consistent with the view that hZTL1 mediates zinc transport across the plasma membrane.

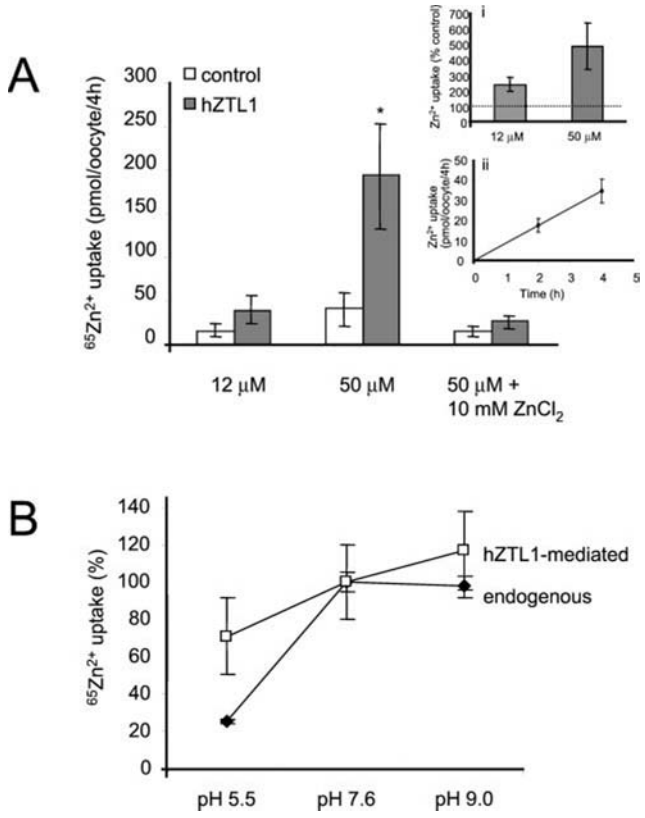

FIG. 5. **Functional expression of hZTL1 in *X. laevis* oocytes.** All data are expressed as the mean ± S.E. for $n = 8–10$ oocytes in each experiment. *A*, uptake of $^{65}Zn^{2+}$ from a solution containing 12 or 50 μM $ZnCl_2$ over 4 h by control oocytes (water-injected or uninjected) compared with hZTL1-injected oocytes; *, $p < 0.05$ by Student's *t* test. Data are pooled; $n = 4$ experiments for 12 μM $ZnCl_2$, and $n = 3$ experiments for 50 μM $ZnCl_2$. In all individual experiments uptake by hZTL1-injected oocytes was significantly greater than by control oocytes ($p < 0.05$ by Student's *t* test). Over a number of experiments we observed no difference in rates of endogenous Zn^{2+} uptake between water-injected and uninjected oocytes. *Inset i*, data expressed as percentage of Zn^{2+} uptake by control oocytes. *Inset ii*, time course for hZTL1-mediated Zn^{2+} uptake by oocytes at 12 μM $ZnCl_2$. Uptake into water-injected controls has been subtracted. *B*, the effect of extracellular pH on uptake from a solution containing 12 μM $ZnCl_2$ of $^{65}Zn^{2+}$ by *X. laevis* oocytes injected with hZTL1 cRNA and by water-injected controls. Net hZTL1-mediated uptake (*i.e.* uptake by hZTL1 cRNA-injected oocytes minus uptake by water-injected controls) is shown. All data are presented as the percentage of uptake measured at pH 7.6.

Although hZTL1-induced zinc uptake appears modest in comparison with endogenous values for oocyte zinc transport, the level of stimulation is commensurate with the apparent activity of the macrophage zinc transporter Nramp1 when expressed in *Xenopus* oocytes (23). Potential mechanisms other than direct hZTL1-mediated flux across the oocyte plasma membrane that might result in increased zinc uptake are stimulation of endogenous plasma membrane zinc transport mechanisms or influx by mass action after hZTL1-mediated intracellular sequestration. Both possibilities can be excluded on the basis that endogenous and hZTL1-stimulated zinc uptake have distinct pH profiles. The observed increase in hZTL1-mediated Zn^{2+} uptake between 12 and 50 μM indicates a high K_m. Based on an estimate of 2.5 liters as the volume of fluid passing through the intestine daily (42) and an average daily intake of 12 mg of zinc (43), we calculate the zinc concentration of the intestinal lumenal contents after a meal to be in the order of 100 μM, commensurate with a low affinity uptake mechanism.

Calculation of intracellular oocyte zinc concentration after hZTL1-mediated Zn^{2+} transport indicates that uptake is accumulative. Most intracellular zinc, however, is protein-bound (44); thus, any calculated apparent intracellular accumulation of Zn^{2+} may be an overestimate. Failure to identify a nucleotide binding motif in the peptide sequence of hZTL1 indicates that ion coupling rather than ATP hydrolysis is likely to be the energy source for any net Zn^{2+} transport by the carrier against an electrochemical gradient. A proton electrochemical gradient across the apical plasma membrane of the enterocyte, deriving from the luminal acid pH microclimate adjacent to the brush border membrane (45), provides the energy source for a number of proton-coupled nutrient transporters (16, 46, 47). The nature of the pH dependence of hZTL1-mediated zinc uptake, however, is inconsistent with proton co-transport. The small observed increase in uptake at alkaline pH might be due to protonation of specific amino acid residues in the polypeptide chain or to proton countertransport (the latter made energetically favorable by the movement of a positively charged Zn^{2+} species in the direction favored by the membrane potential). Reduced uptake of zinc in the presence of an inwardly directed pH gradient, as shown by our data for hZTL1, was observed also in small intestinal brush border membrane vesicles (18), consistent with the expression of hZTL1 in this membrane and a role in uptake of dietary Zn^{2+} across the apical enterocyte membrane.

The functional data we report confirm that hZTL1 can mediate Zn^{2+} uptake across the plasma membrane. We do not exclude at this stage the possibility that hZTL1 may transport other divalent cations in addition to Zn^{2+}. Detailed functional analysis of the transport properties of hZTL1 will be the focus of future study.

Acknowledgment—We thank Judith Piper for providing excellent technical assistance.

REFERENCES

1. Zhao, H., and Eide, D. (1996) *Proc. Natl. Acad. Sci. U. S. A.* **93,** 2454–2458
2. Zhao, H., and Eide, D. (1996) *J. Biol. Chem.* **271,** 23203–23210
3. Eide, D., Broderius, M., Fett, J., and Guerinot, M. L. (1996) *Proc. Natl. Acad. Sci. U. S. A.* **93,** 5624–5628
4. Gaither, L. A., and Eide, D. J. (2001) *J. Biol. Chem.* **276,** 22258–22264
5. Gaither, L. A., and Eide, D. J. (2000) *J. Biol. Chem.* **275,** 5560–5564
6. Grotz, N., Fox, T., Connolly, E., Park, W., Guerinot, M. L., and Eide, D (1998) *Proc. Natl. Acad. Sci. U. S. A.* **95,** 7220–7224
7. Rogers, E. E., Eide, D. J., and Guerinot, M. L. (2000) *Proc. Natl. Acad. Sci. U. S. A.* **97**, 12356–12360
8. Paulsen, I. T., and Saier, M. H., Jr. (1997) *J. Memb. Biol.* **156,** 99–103
9. Kamizono, A., Nishizawa, M., Teranishi, Y., Murata, K, and Kimura, A. (1989) *Mol. Gen. Genet.* **219,** 161–167
10. Conklin, D. S., McMaster, J. A., Culbertson, M. R., and Kung, C. (1992) *Mol. Cell. Biol.* **12,** 3678–3688
11. Palmiter, R. D., and Findley, S. D. (1995) *EMBO J.* **14,** 639–649
12. Palmiter, R. D., Cole, T. B., and Findley, S. D. (1996) *EMBO J.* **15,** 1784–1791
13. Palmiter, R. D., Cole, T. B., Quaife, C. J., and Findley, S. D. (1996) *Proc. Natl. Acad. Sci. U. S. A.* **93,** 14934–14939
14. Huang, L., and Gitschier, J. (1997) *Nat. Genet.* **17,** 292–297
15. Liuzzi, J. P., Blanchard, R. K., and Cousins, R. J. (2001) *J. Nutr.* **131,** 46–52
16. Gunshin, S., Mackenzie, B., Berger, U. V., Gunshin, Y., Romero, M. F., Boron, W. F., Nussberger, S., Gollan, J. L., and Hediger, M. A. (1997) *Nature* **388,** 482–488
17. Tandy, S., Williams, M, Leggett, A., Lopez-Jimenez, M., Dedes, M., Ramesh, B., Srai, S. K., and Sharp, P. (2000) *J. Biol. Chem.* **275,** 1023–1029
18. Tacnet, F., Lauthier, F., and Ripoche, P. (1993) *J. Physiol. (Lond.)* **465,** 57–72
19. Barnes, P. M., and Moynahan E. J. (1973)) *Proc. R. Soc. Med.* **66,** 327–329
20. McMahon, R. J., and Cousins, R. J. (1998) *Proc. Natl. Acad. Sci. U. S. A.* **95,** 4841–4846
21. Murgia, C., Vespignani, I, Cerase, J., Nobili, F., and Perozzi, G. (1999) *Am. J. Physiol.* **277,** G1231–G1239
22. Milon, B., Dhermy, D., Poutney, D., Bourgeois, M., and Beaumont, C. (2001) *FEBS Letts.* **507,** 241–246
23. Goswami, T., Bhattacharjee, A., Babal, P., Searle, S., Moore, E., Li, M., and Blackwell, J. (2001) *Biochem. J.* **354,** 511–519
24. Vidal, S. M., Malo, D., Vogan, K., Skamene, E., and Gros, P. (1993) *Cell* **73,** 469–485
25. Peter, G. J., Davies, A., Watt, P. W., Birrell, J., and Taylor, P. M. (1999) *Biochem. J.* **343,** 169–176
26. Altschul, S. F., Gish, W., Miller, W., Myers, E. W., and Lipman, D. J. (1990) *J. Mol. Biol.* **215,** 403–410
27. Hofmann, K., and Stoffel, W. (1993) *Biol. Chem.* **374,** 166
28. Apweiler, R., Attwood, T. K., Bairoch, A., Bateman, A., Birney, E., Biswas, M., Bucher, P., Cerutti, L., Corpet, F., Croning, M. D. R., Durbin, R., Falquet, L., Fleischmann, W., Gouzy, J., Hermjakob, H., Hulo, N., Jonassen, I, Kahn, D., Kanapin, A., Karavidopoulou, Y., Lopez, R., Marx, B., Mulder, N. J.,

Oinn, T. M., Pagni, M., Servant, F., Sigrist, C. J. A., and Zdobnov, E. M. (2000) *Nucleic Acids Res.* **29,** 37–40
29. Hansen, J. E., Lund, O., Tolstrup, N., Gooley, A. A., Williams, K. L., and Brunak, S. (1998) *Glycoconj. J.* **15,** 115–130
30. Nielsen, H., Engelbrecht, J., Brunak, S., and von Heijne, G. (1997) *Protein Eng.* **10,** 1–6
31. Solovyev, V. V., Salamov, A. A., and Lawrence, C. B. (1995) in *Proceedings of the Third International Conference on Intelligent Systems for Molecular Biology* (Rawling, C., Clark, D., Altman, R., Hunter, L., Lengauer, T., and Wodak, S., eds) pp. 367–375 , AAAI Press, Cambridge, England
32. Solovyev, V. V., Salamov, A. A., and Lawrence, C. B. (1994) *Nucleic Acids Res.* **22,** 5156–5163
33. Persson, B., and Argos, P. (1996) *Protein Sci.* **5,** 363–371
34. Heuchel, R., Radtke, F., Georgiev, O., Stark, G., Aguet, M., and Schaffner, W. (1994) *EMBO J.* **13,** 2870–2875
35. Andrews, G. K., Lee, D. K., Ravindra, R., Lichtlen, P., Sirito, M., Sawadogo, M., and Schaffner, W. (2001) *EMBO J.* **20,** 1114–1122
36. Wang, K., Pugh, E. W., Griffen, S., Doheny, K. F., Mostafa, W. Z., al-Aboosi, M. M., el-Shanti, H., and Gitschier, J. (2001) *Am. J. Hum. Genet.* **68,** 1055–1060
37. Li, L., and Kaplan, J. (2001) *J. Biol. Chem.* **276,** 5036–5043
38. Pinto, M., Robine-Leon, S., Appay, M. D., Kedinger, M., Triadou, N., Dussaulx, E., Lacroix, B., Simon-Assmann, P., Haffen, K., Fogh, J., and Zweibaum, A. (1983) *Biol. Cell* **47,** 323–330
39. Hidalgo, I. J., Raub, T. J., and Borchardt, R. T. (1989) *Gastroenterology* **96,** 736–749
40. Walker, D., Thwaites, D. T., Simmons, N. L., Gilbert, H. J., and Hirst, B. H. (1998) *J. Physiol.* (*Lond.*) **507,** 697–706
41. Langmade, S. J., Ravindra, R., Daniels, P. J., and Andrews, G. K. (2000) *J. Biol. Chem.* **275,** 34803–34809
42. Passmore, R., Meiklejohn, A. P., Dewan, A. D., and Thow, R. K. (1955) *Br. J. Nutr.* **9,** 20–27
43. Van Dokkum, W. (1995) *Nutr. Res. Rev.* **8,** 271–302
44. Outten, C. E., and O'Halloran, T. V. (2001) *Science* **292,** 2488–2492
45. Lucas, M. (1983) *Gut* **24,** 734–739
46. Fei, Y-J., Kanai, Y., Nussberger, S., Ganapathy, V., Leibach, F. H., Romero, M. F., Singh, S. K., Boron, W. F., and Hediger, M. A. (1994) *Nature* **368,** 563–566
47. Thwaites, D. T., and Stevens, B. C. (1999) *Exp. Physiol.* **84,** 275–284